Sol-gel Synthesis of $CaZnAl_2O_4$ Ceramic Nanoparticles and Investigation of their Properties

Sekhar Didde[1,3], R. S. Dubey[2*,] and Sampad Kumar Panda[3]

[1]*Department of ECE, Swarnandhra College of Engineering and Technology, Narsapur, Andhra Pradesh, 534275, India*

[2]*Department of Nanotechnology, Swarnandhra College of Engineering and Technology, Narsapur, Andhra Pradesh, 534275, India*

[3]*Department of ECE, KoneruLaksmaiah Education Foundation, Greenfields, Vaddeswaram, Guntur, Andhra Pradesh, India*

**Corresponding Author: rag_pcw@yahoo.co.in*

Abstract

Dielectric ceramic materials are well-recognized in the semiconductor industry because of their exceptional thermal stability, chemical resistance, and crystallinity. Despite their potential applications, these are also demanded in wireless communication. This paper reports the structural, morphological, and dielectric properties of sol-gel-derived $CaZnAl_2O_4$ ceramic nanoparticles. X-ray diffraction (XRD) analysis exhibited the polycrystalline characteristic of the $CaZnAl_2O_4$ nanoparticles with their crystallite size of 13 nm. Fourier-Transform infrared spectroscopy (FTIR) analysis confirmed the relevant vibration peaks of various functional groups present in the ceramic nanoparticles. Surface morphology study demonstrated the preparation of spherical grains with their mean diameter of 16 nm. The concentric rings also confirm the crystallinity of the nanoparticles that appeared in the selected area diffraction pattern. Furthermore, dielectric properties investigation showed the variation of dielectric permittivity from 23.76 to 21.67 as a function of increased frequency. Similarly, the dielectric loss is found to decrease from 0.047 to 0.039. As a result, the conductivity increased from 1.324 μS/m to 3.639 μS/m as a function of applied frequency.

Keywords: Ceramics, Nanoparticles, sol-gel method, crystallinity, dielectric properties.

1 Introduction

Telecommunication is the most fantastic escalating field of applied sciences that has acquired the interest of public life in the current era. Trending wireless local area networks are rigged in houses, commercial malls, and offices. An antenna is a device that transmits or receives electromagnetic waves from one point to another. These are the primary elements of any wireless structure. The receiving antenna as a part of the system depends on shifting the electromagnetic waves into their original form. Most antennas are resonant radiators, which operate bi-directionally over a relatively narrow frequency band. It is an actuator that converts electrical energy into electromagnetic energy at the same frequency and plays a vital role in wireless communication.

Currently, multifunctional nanomaterials have got demand in the miniaturization of electronic, optoelectronic, photonic and electrical devices. In general, flame retardant (FR-4) and epoxy glass

are preferred as the antenna substrates, while copper, silver, and other metals are used as the patch materials. However, three significant disadvantages associated with the microstrip patch antennas such as a low gain, less efficiency, and narrow frequency bandwidth are needed to compromise. This exhibits the requirement of dielectric materials with high dielectric permittivity and a low dielectric loss to reduce the size of the antenna (Pandirengan, T. et al., 2016). Practically the microstrip patch antennas (MSAs) are demanded in wireless communication. Deschamps explored the microstrip patch antenna in 1950 while its various applications emerged after the pioneer work of Bob Munson in 1972 (Mittal. et al., 2015). The key features of a microstrip patch antenna include its easy integration, less-weight, low-cost, small-size (Vinnik, D.A. et al., 2021). The MPA needed to be modeled to deal with the dissimilar commonness. The MPA is generally employed as directional antennas in telecommunication and comprises alternating current elements above the floor plane. The dielectric material separates the alternating current component and the ground plane. Basically, MSA is a small band radiator, which is unique in wireless technology (Chinnaguruswamy, B. et al., 2021). Among various antennas, the MSAs are well-suited in industrial and commercial applications due to their straight forward design and inexpensive manufacturing cost (Singh, S. Kumar. J. et al., 2020). Along with the dielectric materials demand, a variant of magnetic-dielectric materials is being explored for fabricating the MPAs (Lopes Matias, J. A. et al., 2021). Further, the researchers reported various types of shapes of the patch for improving the gain and resonant bandwidth (Mukta, Ch. et al., 2021).

The dielectric ceramic materials can be synthesized by using various bottom-up techniques. However, the sol-gel approach is the simplest to prepare the dielectric ceramic composite particles. This technique produced pure nanoparticles with lower sintering temperatures, so it is a low-cost process that consumes less energy (Bokov, D. et al., 2021; Aleksandrova, M. et al., 2020). The spinel zinc aluminate ($ZnAl_2O_4$) nanoparticles have distinct characteristics such as wide energy bandgap and high phosphorescent quantum yield (Hussain, Tanveer. et al., 2017). Various researchers claimed the preparation and characterization of spinel metal oxide by adding or doping transition metal ions and explored the dielectric characteristics (Rahman, Ashiqur. et al., 2015; Jia-Min Wu. et al., 2011). Zinc aluminate ($ZnAl_2O_4$) is well recognized in microwave applications. The choice of this material is due to distinct characteristics like good crystallinity, high thermal capability, and excellent chemical registrant. Zinc aluminate is a spinal structure known as gahnite with its formula AB_2O_4, where A indicates the bivalent cations (Zn, Mg, Cd, and Mn, etc.) with the tetrahedral site. The element B fills the octahedral positions of a close-packed face-centered cubic structure in Fd3m space group symmetry. This B position gets occupied by the desired metal elements. It is composed of close-packed 32 oxygen atoms with cations in tetrahedral and octahedral intermissions in a cubic structure. The $ZnAl_2O_4$ is also employed as a catalyst due to its high thermal stability, large mechanical resistance, and low surface acidity (Haung, Sh. et al., 2020).

Several reports have been published on the synthesis of $ZnAl_2O_4$ nanoparticles using cost-effective chemical routes. The crystallite size of $ZnAl_2O_4$ nanoparticles was found reduced with the increase of the doping concentrations of Cr and Mn. The X-ray diffraction investigation revealed a crystallite size of 23nm (DING, M. et al., 2020). Similarly, the synthesis of Cr-doped $ZnAl_2O_4$ nanoparticles using the sol-gel method was reported. They explored the influence of doping concentration of the Cr on the variation of its crystallite size (Shang-Pan, Huang. et al., 2020). Similarly, another group reported the dielectric characteristics of $ZnAl_2O_4$ doped with Mg.

They noticed the increased grain size, which was attributed to the ionic radius of the dopant. The dielectric permittivity of the Mg-$ZnAl_2O_4$ was estimated to be 50, further found increased with the increased doping concentration of Mg (Hussain, Tanveer. et al., 2017). The so-gel-derived $ZnAl_2O_4$ nanoparticles having their crystallite size of 19.92nm were studied. The dielectric properties analysis using the LCR meter showed dielectric permittivity of 8.7. The microstrip patch antenna made-up of these nanoparticles showed return loss of-25.4dB at the resonant frequency of 12.78GHz (Rahman, Ashiqur. et al., 2015). The hydrothermal method was employed to prepare the Mn-doped $ZnAl_2O_4$ nanoparticles, and various properties were studied. The average crystallite size of Mn-doped $ZnAl_2O_4$ nanoparticles was 13nm which further decreased with the increased doping concentration of Mn (Haung, Sh. et al., 2020). The impact of Zn doping in $MgAl_2O_4$ was studied and claimed the increased dielectric permittivity from 7.9 to 8.56 with the increased concentration of Zn (Chang Wei Zheng. et al., 2007). The sol-gel prepared $ZnAl_2O_4$ nanoparticles were studied for various investigations, and finally, a prototype microstrip patch antenna for C band communications was demonstrated. They claimed its resonant frequency at 4.64GHz with a return loss of -17.13dB (Srilali, Siragam. et al., 2022).

In this way, by adopting the simple sol-gel method, one can synthesize the nanoparticle of $ZnAl_2O_4$ after doping with various dopants to tune the dielectric propertied for the well-suited application in fabricating the microstrip patch antenna. This paper presents the synthesis of calcium doped $ZnAl_2O_4$ ceramic nanoparticles and studied their structural, morphological, and dielectric properties. Section 2 presents the materials and methods followed in synthesizing ceramic nanoparticles. The characterized results are discussed in section 3. Lastly, the paper is summarized in Section 4.

2 Experimental

2.1 Materials

Aluminum nitrate nonahydrate ($Al(NO_3)_3.9H_2O$, Sigma-Aldrich), Zinc acetate dehydrate ($Zn(O_2CCH_3)_2.2H_2O$,Lobychem), Ethylene glycol ($C_2H_6O_2$, SdFine), calcium nitrate tetra hydrate ($Ca(NO_3)_2H_8O_4$, Sigma-Aldrich), nitric acid (HNO_3, Lobychem) and ethanol (C_2H_5OH, Sigma-Aldrich) were used. As the source of Zn, Al, and Ca, the chemicals $Zn(O_2CCH_3)_2.2H_2O$,$Al(NO_3)_3.9H_2O$, and $Ca(NO_3)_2H_8O_4$ were used.

2.2 Synthesis & Characterization

First, aluminum nitrate nonahydrate was mixed in 60 ml ethanol with a constant stirring of 5 min. Then 9.906 gm zinc acetate dehydrate and 0.498 ml ethylene glycol were added to the above-prepared solution, which acted as the chelating agent. Later 1.419 gm calcium nitrate tetrahydrate was added. The obtained solution was kept for 1hr stirring at a temperature of 75°C, and further 0.36 ml nitric acid was added to maintain the homogeneity of the solution. After so, the solution was thermally treated at 75^0C for 1 hr. After getting the gel, it was dried at 180 °C for 2 hr and calcined in a muffle furnace at 800°C. The calcined sample was ground for obtaining powder of $CaZnAl_2O_4$. **Fig.**1 depicts the sol-gel process of the $CaZnAl_2O_4$ ceramic nanoparticles as shown here in the first raw. At first, the raw materials were mixed in the beaker at room temperature under a constant stirrer. The solution was kept at temperature 75°C on a magnetic stirrer for 1 hr during

the process. The second raw (shown in the above picture) illustrates the drying, calcination, and grinding process. For instance, the prepared gel was dried in the oven while maintaining the temperature of 80°C for 2 hr. Later, the sample was calcined in a muffle furnace at temperature 800°C for 30 min and finally ground to obtain the nanoparticles.

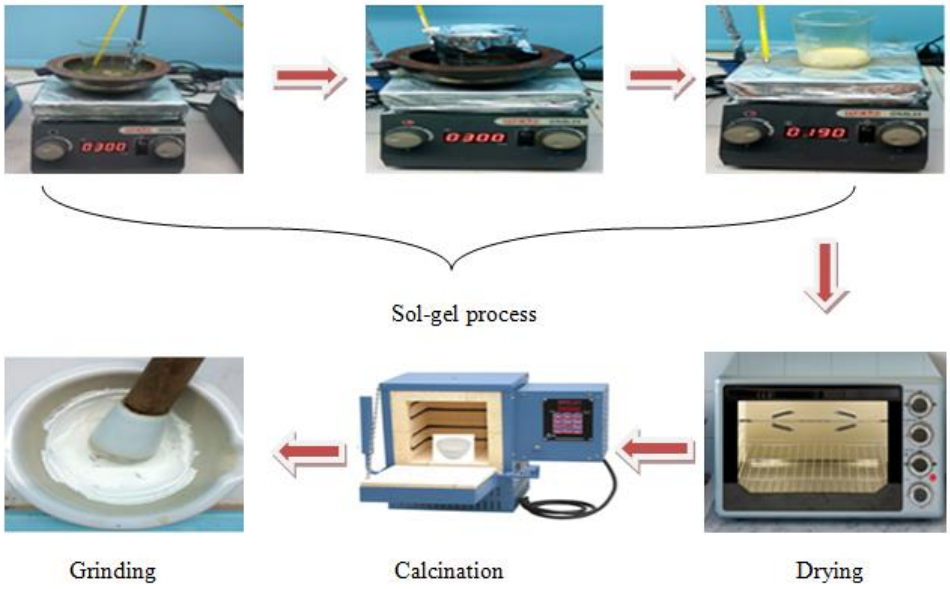

Fig.1: Sol-gel synthesis process of $CaZnAl_2O_4$ nanoparticles.

2.3 X-ray diffraction (XRD)

This technique provides the details of the physical properties of the structure and chemical confirmation of the material under the test. It also gives information on the crystalline types and phases. In this study, we have used an X-ray diffractometer, Bruker D8, Venture.

2.4 Fourier Transform Infrared Spectroscopy (FTIR)

The FTIR is a powerful tool that examines the presence of various chemical bonds in the material. Using this technique, we study the presence of polymers and organic/inorganic substances. Our sample was investigated using FTIR, Perkin Elmer-Spectrum Two, US.

2.5 Transmission Electron Microscopy (TEM)

This technique is used to know the nanoparticles' surface morphology and size distribution. TEM investigation can be done for a tiny sample. We have employed TEM, Talos F200S G2, US in this present work.

2.6 Dielectric Properties

The LCR meter is a technique used to examine the dielectric properties of the specimen. Using this, we study the sample's dielectric permittivity, dielectric loss, conductivity, etc.

3 Results and Discussion

The XRD pattern of $CaZnAl_2O_4$ nanoparticles recorded at 2θ range from 10° to 80° is illustrated in **Fig.2.** We can observe the polycrystalline nature of the synthesized nanoparticles through the XRD pattern.

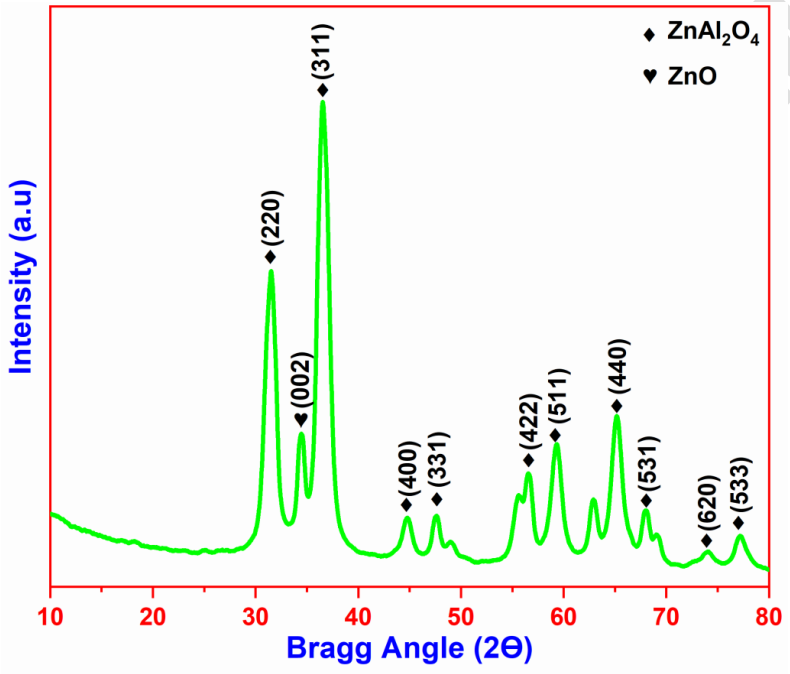

Fig.2: XRD Pattern of $CaZnAl_2O_4$ ceramic nanoparticles.

The diffraction peaks observed at Bragg angle 2θ= 31.80°, 36.41°, 44.76°, 49.11°, 56.55°, 59.37°, 65.15°, 67.98°, 74.01° and 77.22° were ascribed to the planes (220), (311), (400), (331), (422), (511), (440), (531), (620) and (533) respectively. The strong peaks located at 2Θ =31.80° and 36.41° correspond to the face-centered cubic structure of $ZnAl_2O_4$ (R.S. Dubey. et al., 2022; Reem S, Khaleel. et al., 2022). We have also noticed a diffraction peak at 2θ= 34.22° corresponding to the ZnO of the plane (002). The obtained diffraction data was well-matched with the JCPDS File Nos. 00-050-0426 and 36-1451 (Gurugubelli, T. R. et al., 2021; Reem S, Khaleel. et al., 2020). The mean crystallite size of the $CaZnAl_2O_4$ nanoparticles was 13 as computed using Scherrer's equation (Rahman, Ashiqur. et al., 2015). The strong peaks located at 2Θ =31.80° and 36.41° correspond to the face-centered cubic structure of $ZnAl_2O_4$ (R.S. Dubey. et al., 2022; Reem S, Khaleel. et al., 2022). We have also noticed a diffraction peak at 2θ= 34.22° corresponding to the ZnO of the plane (002). The obtained diffraction data was well-matched with the JCPDS File Nos. 00-050-0426 and 36-1451 (Gurugubelli, T. R., et al., 2021; Reem S. Khaleel, et al., 2020). The

mean crystallite size of the $CaZnAl_2O_4$ nanoparticles was 13 as computed using Scherrer's equation (Rahman, Ashiqur. et al., 2015).

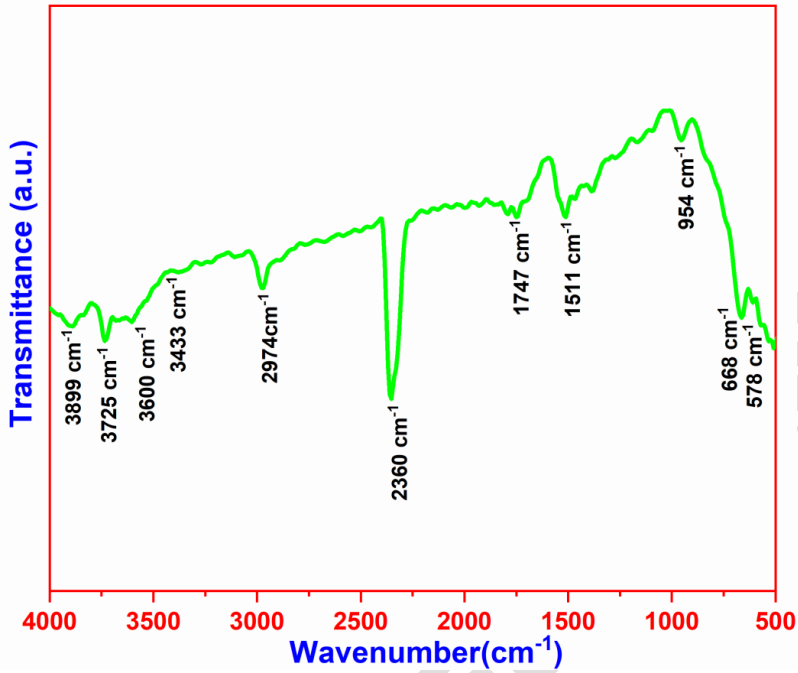

Fig.3: FTIR spectra of $CaZnAl_2O_4$ ceramic nanoparticles.

Fig.3 depicts the Fourier-Transform infrared spectroscopy (FTIR) spectra of $CaZnAl_2O_4$ nanoparticles scanned in the region of 4000 to 500cm^{-1}. The FTIR spectra demonstrates the vibration peaks at wave number values of 578 cm^{-1}, 668 cm^{-1}, 954 cm^{-1}, 1511 cm^{-1}, 1747 cm^{-1}, 2360 cm^{-1}, 2974 cm^{-1}, 3433 cm^{-1}, 3600 cm^{-1}, 3725 cm^{-1} and 3899 cm^{-1}. It can be noticed that the peaks originating at 578 cm^{-1} and 668 cm^{-1} are the characteristic peaks of $ZnAl_2O_4$. The peak at 578 cm^{-1} corresponds to Zn-O bond and while the other one aligned 668 cm^{-1} was attributed to the Al-O bond. The broad absorption band in the wave number range 3433-3899 cm^{-1}. It is found regarded to the stretching vibration of hydroxyl groups, due to the water contents. The band located 2360 cm^{-1} indicates the existence of oxygen bonds. This peak is identified in all spinel compounds related to the grains' spinel structure (Wang, Shi-Fa. et al., 2015). Another peak at 1516 cm^{-1} can be regarded as the stretching vibration of aluminum and oxygen bond. The other vibration peaks in from 500cm^{-1} to 900 cm^{-1} are ascribed to the inorganic network, related to the metal-oxygen, aluminum-oxygen, and metal-oxygen-aluminum stretching frequencies.

Fig.4(a) depicts the TEM micrograph, which exhibits the agglomerated particles of $CaZnAl_2O_4$. **Fig.4(b)** shows another TEM image recorded at the scale of 20 nm, evidenced spherical morphology of $CaZnAl_2O_4$ grains with their average diameter of 16nm. Selected area diffraction pattern (SAED) was recorded to know the crystallinity of the prepared nanoparticles, as shown in **fig.4(c)**. The concentric rings that appeared in the SAED pattern indicate the prepared nanoparticles' crystallinity. This SAED pattern coincided with the XRD results. We have analyzed the compositional elements present in the sample using the EDS measurements. **Fig.4(d)** shows the presence of Zn, Ca, Al and O at energy 1.00 eV, 3.80 eV, 1.50 eV, and 0.50 eV, respectively.

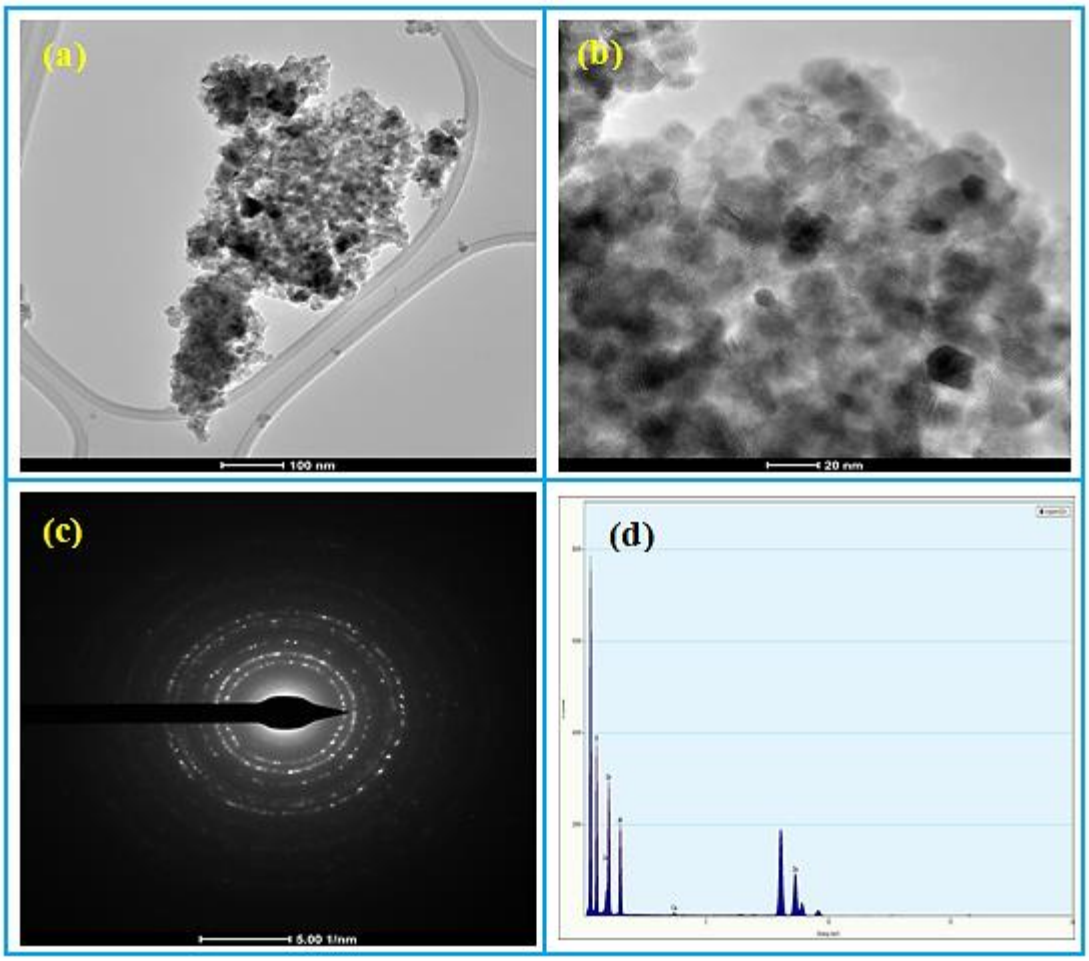

Fig.4: TEM micrographics at the scale of 100 nm (fig.a), at the scale of 20 nm (fig.b), SAED pattern (fig.c) & EDS spectrum (fig.d) of $CaZnAl_2O_4$ceramic nanoparticles.

Fig.5 depicts the dielectric permittivity of the $CaZnAl_2O_4$ ceramic nanoparticles was tested using an LCR meter in the frequency range from 300 KHz to 1MHz. One can notice the change in dielectric permittivity with the increased frequency can be noticed. This evidences the decreased dielectric permittivity with the increased frequency. The dielectric permittivity shows a relatively high value at lower frequencies, with a gradual decrease with the increased frequency. We computed the dielectric permittivity using the simple formula, $\varepsilon_r=(Cd/\varepsilon_r A)$. Here, ε_r is the dielectric permittivity of the sample, C, d are the capacitance, thickness, and cross-sectional area of the pellet. The dielectric permittivity of $CaZnAl_2O_4$ was found to be decreased from 22.92 to 21.66, with the applied frequency from 300 KHz to 1MHz. The sample under the test might have a low electrical resistance compared to the grain boundaries due to its crystalline nature. Grains and grain boundaries behave like two sheets with distinct electrical properties. Maxwell-Wagner interfacial polarization can occur in the grains around the grain boundaries due to the carrier's aggregation around these larger resistant boundaries upon the applied electric field (Hussain, Tanveer. et al., 2017). When the applied frequency is raised, the charge carriers seek to reverse their way and again try to line up one another in the way of the applied field. As these charges try to rest, the polarity of the applied field again changes, and so on. As a result, these charges cannot

find the time they need to rest, increasing frequency decreasing the polarization. So that at a higher frequency, the dielectric constant decreases.

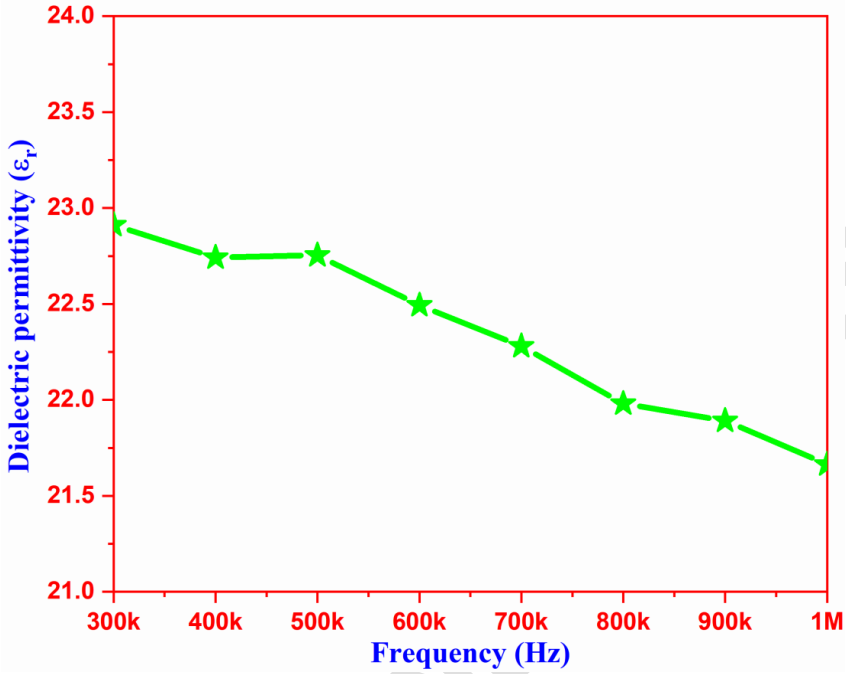

Fig.5: Dielectric permittivity of $CaZnAl_2O_4$ ceramic nanoparticles.

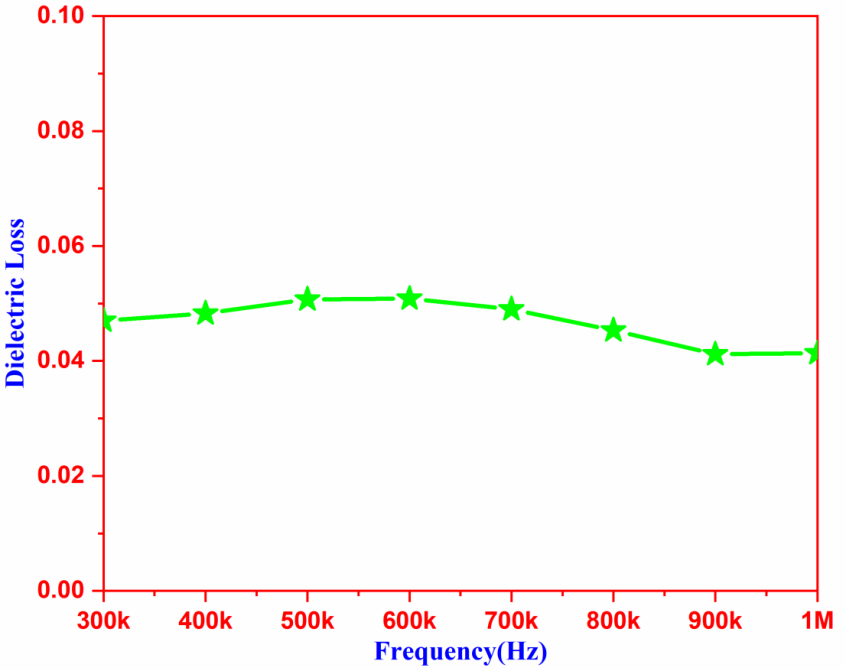

Fig.6: Dielectric loss of $CaZnAl_2O_4$ ceramic nanoparticles.

Dielectric loss refers to the loss of energy in the form of heat due to the movement of charged particles. **Fig.6** shows the dielectric loss of $CaZnAl_2O_4$ nanoparticles in accordance with frequency from 300 KHz to 1 MHz. It can be observed that dielectric loss was increased with decreased frequency, and the dielectric loss was reduced from 0.047 to 0.039 in the applied frequency range from 300 KHz to 1MHz. High energy is necessary for optimal polarization resonance, resulting in increased energy distraction or high energy loss at lower frequencies. While at higher frequencies, resonance occurs freely with a bit of polarization in the grain boundaries, thus, low energy loss can be observed with the increased frequency (Hussain, Tanveer. et al., 2017).

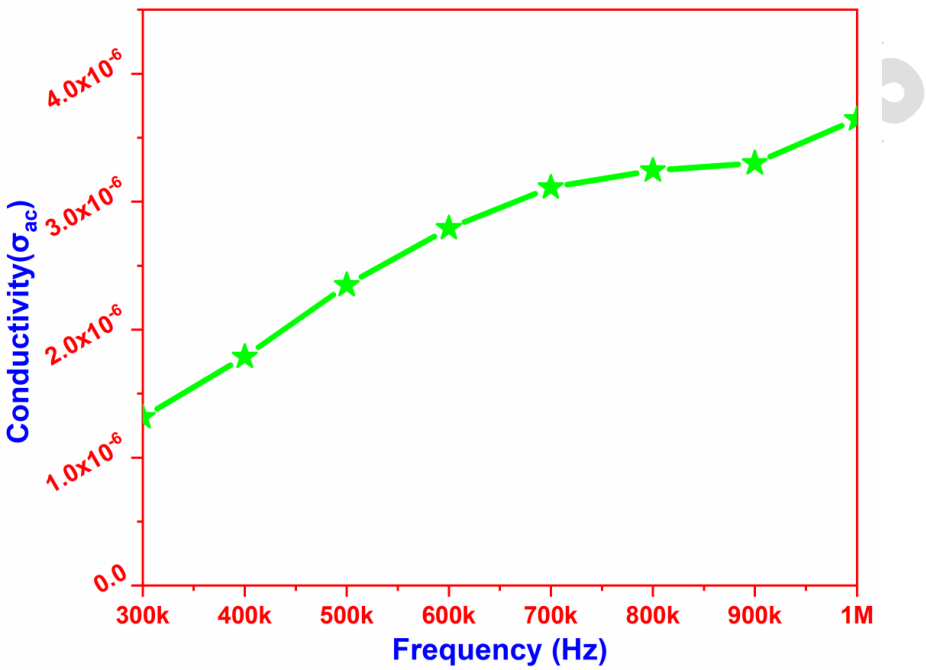

Fig.7: Conductivity of $CaZnAl_2O_4$ ceramic nanoparticles as a function of frequency.

The conductivity of a material indicates its capability to perform electrical current. **Fig.7** shows the frequency-dependent ac conductivity of $CaZnAl_2O_4$ ceramic nanoparticles plotted in the frequency range from 300 KHz to 1MHz at room temperature. We have estimated the ac conductivity using a simple relation $\sigma_{ac}=\omega\varepsilon_0\varepsilon_r\tan\delta$, where ε_0 is the dielectric constant of free space ε_r is the dielectric permittivity of the sample, and $\tan\delta$ is dielectric loss of the material. The material's conductivity depends upon the angular frequency of the applied signal. **Fig.7**, we observed the increased conductivity with the increased applied frequency. The increasing trend of ac conductivity exhibits space charges scattering cations across the adjacent sites (Hussain, Tanveer. et al., 2017). Here, the ac conductivity was increased from 1.324 µS/m to 3.639 µS/m with increased frequency.

4 Conclusions

The prepared $CaZnAl_2O_4$ ceramic nanoparticles were synthesized and studied using various techniques. The XRD investigation endorsed the polycrystalline characteristic of the nanoparticles. The FTIR investigation exhibited the presence of various functional groups

anticipated in the synthesized nanoceramic compound. The TEM study demonstrated the preparation of spherical grains of $CaZnAl_2O_4$ with their mean diameter of about 16nm. The SAED pattern confirmed the polycrystalline structure with the formation of concentric rings. The dielectric permittivity of $CaZnAl_2O_4$ was in the range from 22.92 to 21.66, whereas the dielectric loss was from 0.047 to 0.039. Similarly, conductivity was varied from 1.324 μS/m to 3.639 μS/m with applied frequency. Remarkably, the obtained dielectric permittivity of $CaZnAl_2O_4$ nanoparticles is increased to 22.92. This enhanced characteristic of the ceramic nanoparticles would be suitable in microwave applications such as fabricating the microstrip patch antenna or resonator.

5. References

Aleksandrova. M., Jivov. B., Lakov. L., (2020). Summary of sol-gel synthesis of materials with electronic applications international scientific journal "materials science. non-equilibrium phase transformations". web issn 2534-8477.

Bokov.D., Jalil.T.A.,Chupradit.S., Suksatan.W., Ansari.M.J., Shewael.I.H., Valiev.G.H., Kianfar.E.(2021) Nanomaterial by Sol-Gel Method: Synthesis and Application. Advances in Materials Science and Engineering, Volume 2021, Article ID 5102014, 2

Chang Wei Zheng; Shu Ya Wu; Xiang Ming Chen; Kai Xin Song (2007). Modification of $MgAl_2O_4$ Microwave Dielectric Ceramics by Zn Substitution.,90(5),1483–1486.

Chinnagurusamy, B., &Perumalsamy, M. (2021). Multiband microstrip patch antenna using copper nano radiating element for X band and C band applications. International Journal of Numerical Modelling: Electronic Networks, Devices and Fields.

DING.M; WEI.Z; LI.K; Wu.X; SHI.J; HAUNG.Sh (2020). Influence of Cr and Mn co-doping on the microstructure and optical properties of spinel structured $Zn_{0.95-x}Cr_{0.05}Mn_xAl_2O_4$ nanoparticles, Journal of the Ceramic Society of Japan 128 [11] 927-935.

Gurugubelli, T. R., Babu, B., &Yoo, K. (2021). Structural, Optical, and Magnetic Properties of Cobalt-Doped $ZnAl_2O_4$ Nanosheets Prepared by Hydrothermal Synthesis. Energies, 14(10), 2869.

Huang. Sh; Wei, Zhiqiang; Wu, Xiaojuan; Shi, Jiwen.(2020) Optical properties and theoretical study of Mn doped $ZnAl_2O_4$ nanoparticles with spinel structure. Journal of Alloys and Compounds, 154004

Hussain, Tanveer; Junaid, Muhammad; Atiq, Shahid; Abbas, Syed Kumail; Ramay, Shahid M.; Alrayes, Basel F.; Naseem, Shahzad. (2017) Tunable dielectric behaviour and energy band gap range of $ZnAl_2O_4$ ceramics mediated by Mg substitution. Journal of Alloys and Compounds, 724, 940–950.

Jia-Min Wu; Wen-Zhong Lu; Wen Lei; Xiao-Chuan Wang (2011). Preparation of $ZnAl_2O_4$-based microwave dielectric ceramics and GPS antenna by aqueous gelcasting. , 46(9), 1485–1489.

Lopes Matias, J. A., Silva, I. B. T., Sousa, M. E. T., Oliveira, J. B. L., Morales, M. A., & da Silva, D. R. (2021). $(Bi_{13}Co_{11})Co_2O_{40}$–$Co_3O_4$ nanocomposites: Synthesis, characterization and application as substrate for microstrip patch antenna. Ceramics International.ceramint.2021.04.164

Mittal, N.(2015) Design analysis and fabrication of microstrip patch antennas for various applications using electromagnetic band gap and defected ground structures. Ph.D. thesis, Thapar University, Punjab, India.

Mukta, Ch., Rahman,M., and Islam.A.Z.M.T, (2021). Design of a Compact Circular Microstrip Patch antenna for WLAN applications, International Journal on AdHoc Networking Systems (IJANS) Vol. 11, No. 3.

Pandirengan, Thiruramanathan; Arumugam, Marikani; Durairaj, Madhavan; ThangaiyanadarSuyambulingam, Gokul Raja (2016). Development of performance-improved global positioning system (GPS) patch antenna based on sol-gel-synthesized dual-phase $(Bi_4Ti_3O_{12})_X$-$(CaCu_3Ti_4O_{12})_{1-X}$ composites. Crystal Research and Technology, 51(6), 366–379.

Rahman, Ashiqur; Islam, Mohammad Tariqul; Zulfakar, MohdSyafiq; Abdullah, Huda (2015). Synthesis and characterization of gahnite-based microwave dielectric ceramics (MDC) for microstrip antennas prepared by a sol–gel method. Journal of Sol-Gel Science and Technology, 74(2), 557–565.

Reem S. Khaleel, Mustafa Sh. Hashim, SamerGh. Majeed. (2022) Synthesis of ZnO thin film by chemical spray pyrolysis using its nano powder. Kuwait J.Sci., Vol.49, No.(1).

Reem S. Khaleel, Mustafa Sh. Hashim. (2020) Fabrication of ZnO sensor to measure pressure, humidity and sense vapors at room temperature using the rapid breakdown anodization method, Kuwait J. Sci.47 (1) pp. 42-49.

R. S. Dubey, S. Srilali, Y. T. Ravikiran, G. Satheesh Babu and K. V. Katta (2022). Synthesis and characterization of $Zn_{x-1}Al_2O_4(TiO_2)_x$ nanocomposite ceramics and their humidity sensing properties, J Mater Sci, Composites & nanocomposites.

Shang-Pan, Huang; Zhi-Qiang, Wei; Xiao-Juan, Wu; Ji-Wen, Shi (2020). Optical properties of Cr doped $ZnAl_2O_4$ nanoparticles with Spinel structure synthesized by hydrothermal method. Materials Research Express, 7(1), 015025.

Singh.S, Kumar.J.(2020). A Review Paper on Rectangular Microstrip Patch Antenna National Conference on Industry 4.0(NCI-4.0)

Vinnik, D. A., Zhivulin, V. E., Sherstyuk, D. P., Starikov, A. Y., Zezyulina, P. A., Gudkova, S. A., Trukhanov, A. V. (2021). Electromagnetic properties of zinc–nickel ferrites in the frequency range of 0.05–10 GHz. Materials Today Chemistry, 20, 100460.

Srilali Siragam, R.S.Dubey; Lakshman Pappula.(2022). Investigation of V_2O_5-$ZnAl_2O_4$ Composite Nanoparticles for C-band Microstrip Patch Antenna Applications, Kuwait Journal of Science, 10.48129/kjs. 17783

Wang, Shi-Fa; Sun, Guang-Zhuang; Fang, Lei-Ming; Lei, Li; Xiang, Xia; Zu, Xiao-Tao (2015). A comparative study of $ZnAl_2O_4$ nanoparticles synthesized from different aluminum salts for use as fluorescence materials. Scientific Reports, 5, 12849.